NOTE

Numerical Correlation for Thermal Conduction in Packed Beds

KURT O. LUND[*1], *HUY NGUYEN*[1], *STEPHEN M. LORD*[2] *and CHRYSTAL THOMPSON*[2]

[1] *Department of Mechanical and Aerospace Engineering, Jacobs School of Engineering, Center for Energy and Combustion Research, University of California, La Jolla, CA 92093-0411*

[2] *SML Associates, 109 Peppertree Lane, Encinitas, CA 92024*

The numerical conduction of heat in packed beds of particles is investigated, including the effects of inter-particle microasperity gaps and deformation contacts. A detailed numerical model of two half spheres in contact with interstitial fluid is constructed, including asperity (roughness) gaps and deformation contacts on the respective orders of 5 μm and 100 μm for 1 mm particle diameters. The resulting heat flux distributions at the diametrical planes of the particles are integrated to yield the overall thermal conductance, K, or resistance, $R = 1/K$, between the two diametrical planes. The results show K to be strongly dependent on the interstitial fluid gap and the deformation contact diameter, as well as on fluid and solid conductivities. The effective bed conductivity, k_e, is determined as a function of K and the void fraction, and correlated in terms of bed parameters. The resulting k_e correlation agrees well with published experimental data over a wide range of substances and temperatures.

On étudie la conduction numérique de la chaleur dans des lits garnis de particules, incluant les effets des écarts de microaspérité inter-particules et les contacts de déformation. Un modèle numérique détaillé de deux demi-sphères en contact avec un fluide interstitiel est mis au point, qui inclut les aspérités (rugosité) et les contacts de déformation respectivement de 5 μm et 100 μm pour des diamètres de particules de 1 mm. Les distributions de flux de chaleur résultant dans le plan diamétral des particules sont intégrées afin d'établir la conductance thermique, K, ou la résistance, $R = 1/K$, entre les deux plans diamétrals. Les résultats montrent que K est fortement dépendant de l'espace fluide interstitiel et du diamètre de contact de déformation, et des conductivités du fluide et des solides. La conductivité effective du lit, k_e, est déterminée en fonction de K et de la fraction de vide et corrélée en termes de paramètres de lit. La corrélation k_e résultante concorde bien avec des données expérimentales publiées pour une vaste gamme de substances et de températures.

Keywords: conduction, radiation, packed beds, thermal, effective conductivity, correlation, particle contact.

Popular bed conduction models, based on axial 1-D conduction in the sphere and interstitial fluid, were developed by Yagi and Kunii (1957), Dixon (1985), and Hayashi, et al. (1987). More exact analyses using radial and angular conduction, with solutions by relaxation methods, were performed by Deissler and Boegli (1958), Krupiczka (1967), and by Wakao and Kato (1969). A harmonic method was used by McPhedran and McKenzie (1978) for spheres in very close proximity, but not touching. Chan and Tien (1973) considered contacting spheres in vacuum, with Hertzian contact deformation, whereas Wakao and Kato (1969) used 1-D conduction at the contact point, but without size variation of the contact region. Batchelor and O'Brien (1977) investigated theoretically both contacting and non-contacting spheres for thermal and electrical conduction. In the present paper, the emphasis is on simple, but widely applicable, correlations based on numerical analysis.

Although thermal contact conductance is recognized as important, its effect appears not to be included in practical correlations, nor is the effect of micro-asperities. These depend on surface oxides, on surface roughness, and on the deformation contact area relative to the particle size as discussed by Yovanovich (1967). Theoretically, the area can be determined by the Hertz contact theory with the loads and solid properties known, as by Balakrishnan and Pei (1979) and Chan and Tien (1973); however, this information is frequently not available, and the effect must usually be determined by comparison with experiment as suggested by Bauer and Schluender (1978). Effects of deformation contact was considered by Lund et al. (1997).Reviews of correlations and chemical engineering applications are by Kulkarni and Doraiswamy (1980), Specchia et al. (1980), and by Lemcoff et al. (1990); other applications are in fusion reactor design (Kamiuto, 1990, 1991, Gorbis et al., 1995, Mingjie et al., 1995), in thermal insulation (Chan and Tien, 1973), and in porous media (Kaviany, 1995).

Experimentally, the effective conductivity for packed beds has been measured for various powders by Deissler and Boegli (1958), by Fukai et al. (1990), for aluminum oxide, and more recently by Tavman (1996) for sand grains. In the millimeter size range, packed bed heat transfer was measured by Melanson and Dixon (1985), and by Huber and Jones (1988).

In the present work, two contacting spheres are modeled as in Figure 1, with constant temperatures specified on the two diametrical planes shown. This results in a detailed heat flow field within the particle which is decidedly non-axial but converges to the point of minimum separation between the two particles; the resulting heat flux at the diametrical planes is then area integrated to yield the overall heat flow and conductance, K, for the region.

To accomplish this, a finite element numerical model is constructed as shown in Figure 2, where the smallest elements are on the order of 2% of the particle diameter (i.e., 20 μm for a 1 mm particle); contact conductance is modeled by setting the conductivity of several of the smallest fluid elements to the solid value.

*Author to whom correspondence may be addressed. E-mail address: lund@ames.ucsd.edu

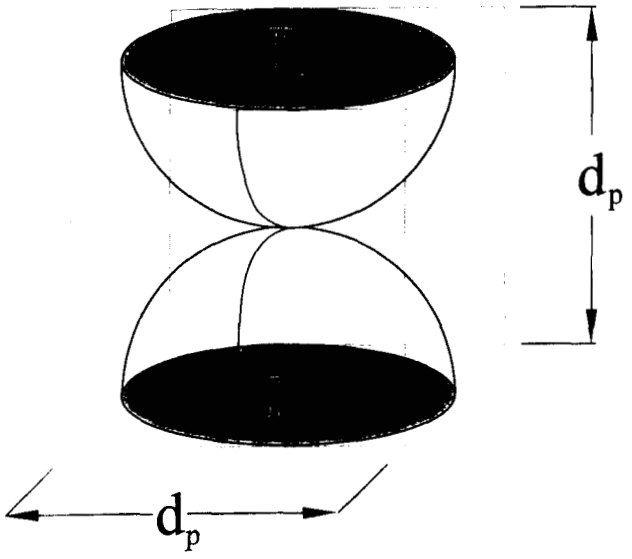

Figure 1 — Contacting spheres and unit cell.

The contacting particle conductance, K, is determined generally for fluid/solid conductivity ratios < 1; however, by limiting this ratio to small values (i.e., gases with solid particles) the numerical results generated for K between two particles is extended analytically to the face centered and body centered packing arrangements and their void fractions, thus leading to a general correlation of the effective conductivity, k_e, for the packed bed.

Analysis

Finite element model

The FE model consists of the two half spheres in close proximity, as in Figure 1, with temperatures of 1°C and 0°C specified at the lower and upper diametrical planes, respectively. This unit temperature difference of ΔT = 1°C was chosen for convenience in application of the COSMOS FE program. Similarly, the solid conductivity was taken as k_s = 1 W/mK, and the "particle" diameter as d_p = 1 m; fluid conductivities were varied from k_f = 1 μ W/m·K to 1 W/m·K. About 1600 elements were used as shown in Figure 2.

The interface gap in Figure 2 varied from 1 mm to 5 mm at the centerline, relative to the 1 m particle. For a 1 mm particle this gap is only 1 to 5 μm, which is comparable to typical surface roughness heights; for k_f = 0.02 W/m·K, this corresponds to unit surface conductances of 20 000 to 4 000 W/m^2·K, which are comparable to the contact conductances between flat surfaces. Thus, the numerical model is sufficiently detailed to account for normally experienced contact conductance.

The effect of contact was modeled by increasing the gas conductivity of the center-most gap elements to the solid value, thus modeling micro asperity deformation contact or micro-welding of the two particles at the contact point. This process yields the normal diametrical heat fluxes shown in Figure 3, where the lowest curves (d_c = 0) are for gas gaps, and the others are for the percent contact diameters shown. It is seen that the fluxes are higher near the centerline where there is a shorter conductance distance to the gap, and that the flux increases with percent contact diameter; however, the heat flow through a ring of width Δr increases with radius, r. By area integration of the flux profiles in Figure 3,

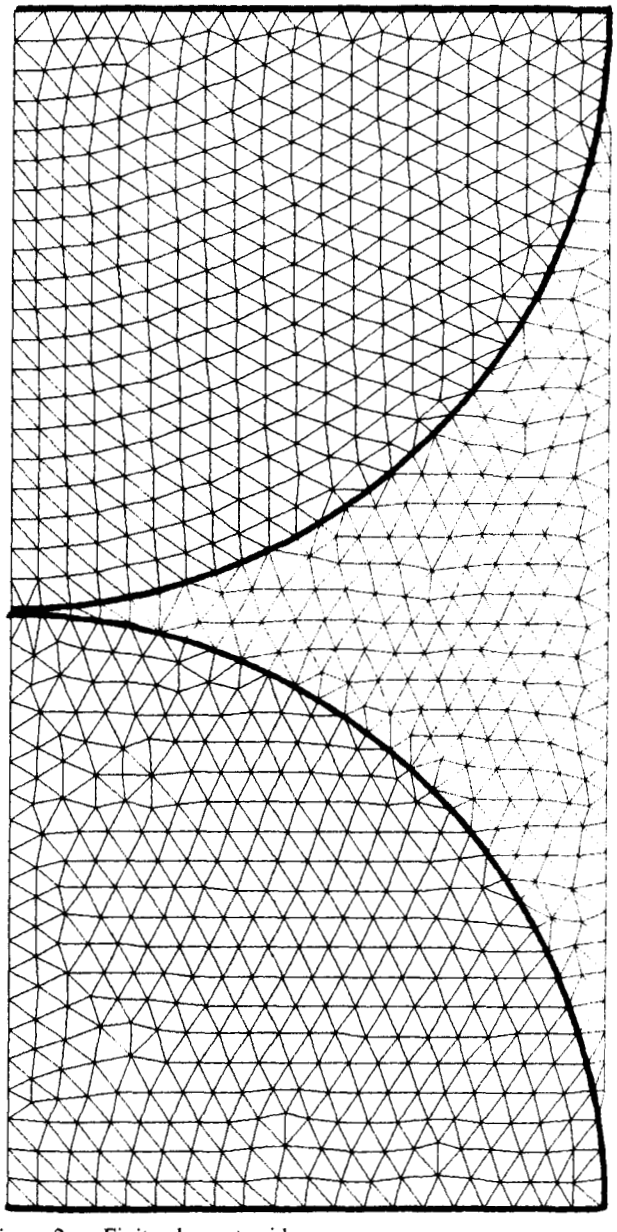

Figure 2 — Finite element grid.

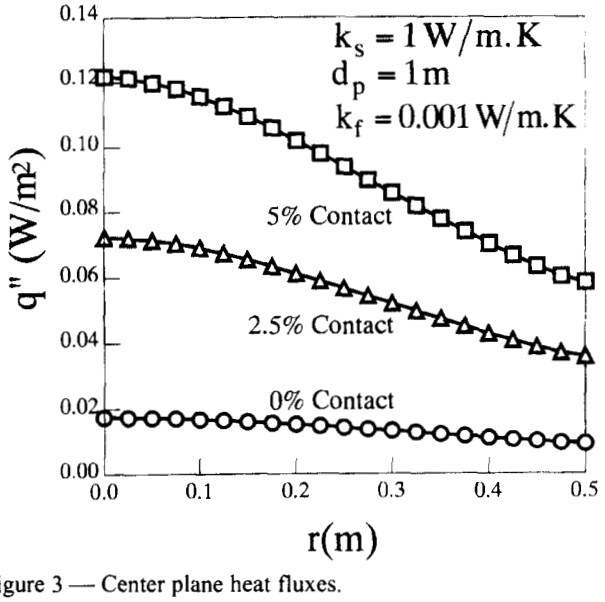

Figure 3 — Center plane heat fluxes.

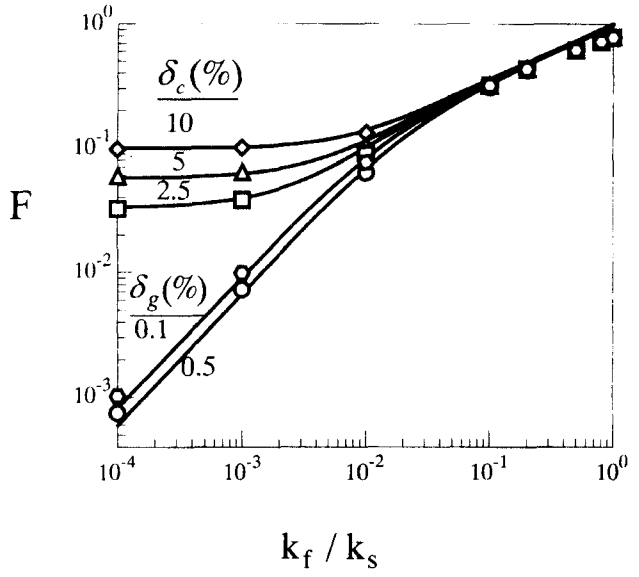

Figure 4(a) — Summary of numerical conductance data.

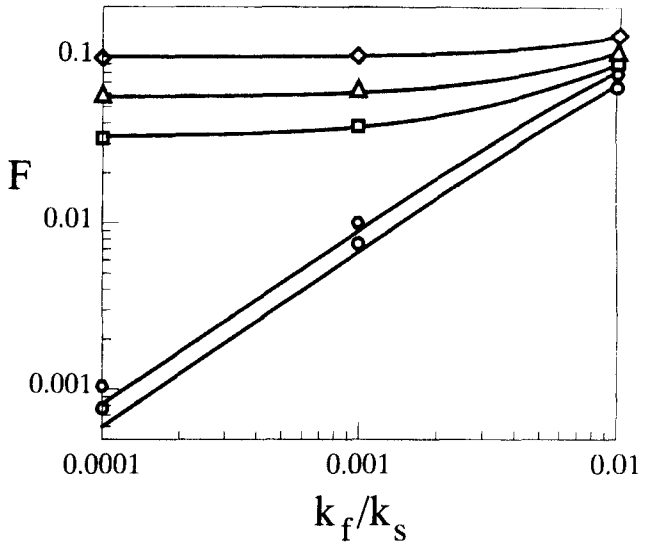

Figure 5 — Comparison of correlation with numerical data.

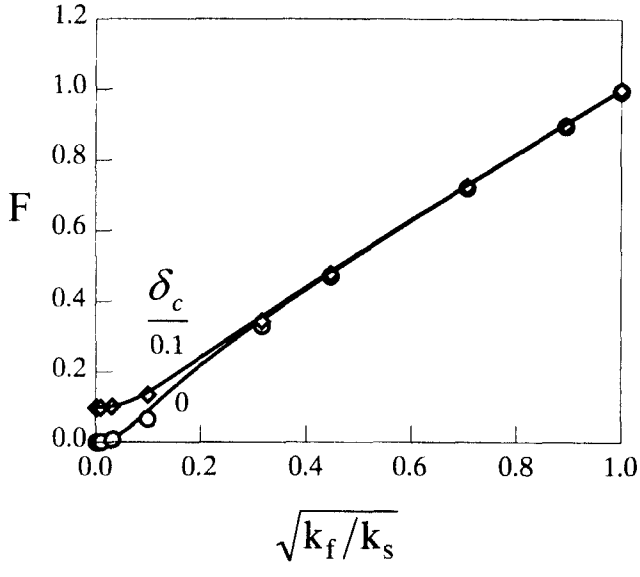

Figure 4(b) — Variation of cell conductance with conductivity ratio.

the integrated heat rates Q and the overall, plane-to-plane conductances $K = Q/\Delta T$ (or the resistances, $R = \Delta T/Q$) are obtained.

Finite element numerical data

Figure 4a summarizes the above numerical data where $F \equiv K/d_p k_s$ is plotted versus $\kappa \equiv k_f/k_s$, with the contact-diameter and particle-gap ratios as parameters: $\delta_c \equiv d_c/d_p$ and $\delta_g \equiv g/d_p$. In this log-log plot, which is normalized by k_s and $d_p k_s$, two similar "zero-contact" curves are shown for inter-particle gaps of 0.1% and 0.5% of the particle diameter, which reflect the average micro-proximity of the two particles. Because of surface roughness, there will always be some gas gap between particles; therefore, the effective conductivity will depend on the particle surface roughness as well as on the interstitial fluid conductivity. For example, for normally-rough sub-millimeter particles, nano-scale contacts would occur before the average gap could become as small as 1 μm; however, such undeformed nano-contacts are too small to contribute significantly to the heat transfer occurring through the micro-scale fluid gap. Larger fluid gaps (i.e., a matrix with solid inclusions) were considered by McPhedran and McKenzie (1978), but are not of interest in this article.

When a particle bed is loaded, either mechanically or by particle weight, elastic deformations can occur from Hertzian stresses between particles. Such deformation effects are included in Figure 4a as effective contact diameter ratios between particles, δ_c. As $\kappa \to 0$, the deformation-contact curves approach constant values as the heat transfer is concentrated in the deformation region, whereas for no deformation the curves diminish linearly as the heat transfer is proportional to the fluid conductivity. As $\kappa \to 1$, all curves approach the same function because with the same solid and fluid conductivities the effect of relative magnitudes disappears (in Figure 4a, $K/d_p k_s \to 1$ as $k_f/k_s \to 1$, as expected, because simple fluid conduction for the cell corner regions outside the sphere was included). This is seen more clearly in Figure 4b, which is a linear plot of $K/d_p k_s$ versus $\sqrt{\kappa}$; it appears that, to an excellent approximation, the inter particle conductance varies linearly with the square root of the fluid conductivity for large κ's for all surface conditions. However, for gases with metallic solids the conductivity ratio is usually small with significant effects of δ_c and δ_g. A similar variation was found by Batchelor and O'Brien (1977).

Effective conductivity correlation

The results in Figures 4 show that for high κ each of the curves converge to the same function which varies approximately as $\sqrt{\kappa}$, and that for low κ the curves are either linear with κ or approach a constant. Therefore, each of the curves can be adequately fitted by the fractional form:

$$F \equiv \frac{K}{d_p k_s} = \frac{a + b\kappa(1 + c\sqrt{\kappa})}{1 + d\kappa} \quad \ldots\ldots\ldots\ldots\ldots\ldots \quad (1)$$

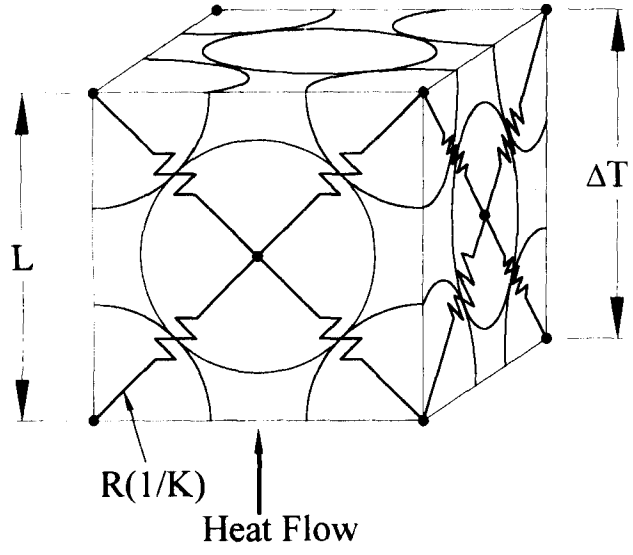

Figure 6 — Conductance for the FCC cell.

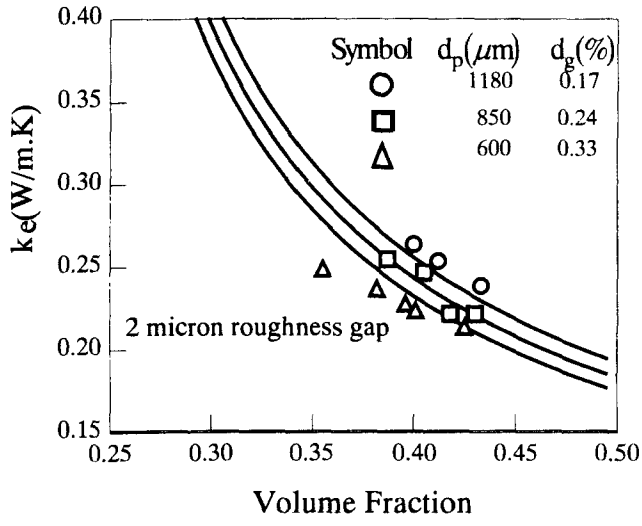

Figure 7 — Comparison with sand-grain data.

where a to d are fitting parameters, where $a(\delta_c)$ accounts for the effect of contact deformation and $b(\delta_g)$ accounts for the effect of inter particle gaps. For small a and for large c and d it is clear that $F \rightarrow \sqrt{\kappa}$ as $\kappa \rightarrow 1$, and that $F \rightarrow a + b\kappa$ as $\kappa \rightarrow 0$, which are the correct limits for the generated data; to satisfy $F(1) = 1$ we take $d = b(1 + c) - 1$. By extensive data manipulation, an excellent fit to all data is given by:

$$F \equiv \frac{K}{d_p k_s} = \frac{0.63\delta_c^{0.8} + 1.9\delta_g^{-0.2}\kappa(1+9\sqrt{\kappa})}{1+(19\delta_g^{-0.2}-1)\kappa};$$

$$0.001 \le \delta_g \le 0.005 \quad \ldots\ldots\ldots\ldots\ldots\ldots\ldots\ldots \quad (2)$$

This variation with δ_c is similar to the previous analysis (Lund, et al., 1997); by comparison, Balakrishnan and Pei (1979) found a linear increase of K with d_c. Equation (2) is compared with the numerical data in Figure 5 for a practical range of κ, and was also used for the solid lines in Figures 4. The agreement of the correlation is excellent.

Effective conductivity

The above results for low conductivity ratios, k_f/k_s, show that the spheres are largely isothermal over their respective volumes, with a significant gradient in the gas between them, or near the contact point. Because of this, these results are insensitive to the orientation of the specified diametrical temperature planes, and the present model is accurate for particles in a 3-D array where $\kappa < 0.1$.

The effective bed conductivity is obtained from the total heat transfer through cell area A and over length L: $Q_T = (k_e/L)\, A\, \Delta T$. For several types of particle packing cells, such as the FCC in Figure 6, this formula led to $k_e/m = K/d_p$, where k_e is the effective bed conductivity, and m is listed in Table 1 for several types of packing arrangements (Chan and Tien, 1973, Batchelor and O'Brien, 1977):

Table 1
Effect of Packing Arrangements

Cell Type	Packing	Void,	m
Simple Cubic	52.36%	47.64%	$1 = 1.0$
Body Center Cubic	68.02%	31.98%	$3^{1/2} = 1.732$
Face Center Cubic	74.05%	25.95%	$2 \times 2^{1/2} = 2.828$

Thus, there is an increase in k_e with solid packing fraction, as expected. The exact packing pattern at any location in a packed bed is not known, and will vary between these and other patterns, and with the sphericity of the particles; therefore an averaged packing will be used in practice. From the above table a correlation of m vs. ε is as follows:

$$m = 0.393/(\varepsilon - 0.2)^{0.7} \quad \ldots\ldots\ldots\ldots\ldots\ldots \quad (3)$$

Therefore, the correlation for effective bed conductivity for $k_s >> k_f$ is the following:

$$k_e = \frac{0.393k_s}{(\varepsilon-0.2)^{0.7}} \times \frac{0.63\delta_c^{0.8} + 1.9\delta_g^{-0.2}(k_f/k_s)(1+9\sqrt{k_f/k_s})}{1+(19\delta_g^{-0.2}-1)(k_f/k_s)} \quad \ldots\ldots\ldots\ldots\ldots\ldots\ldots\ldots \quad (4)$$

In this correlation, δ_g is always > 0, even when there is deformation contact and $\delta_c > 0$.

Comparison of results

For variously packed sand grains in air, Tavman (1996) measured void fraction, particle-diameter ranges, and solid and bed-effective conductivities. In Figure 7, the above correlation is compared to these experiments for an assumed roughness gap of $g = 2$ μm. Considering that this is the only adjusted factor, and that the correlation (4) was determined by purely numerical and analytical means, the agreement between theory and experiment is remarkable. The general variation of k_e with ε corresponds to previous results (Krupiczka, 1967), and k_e is seen to increase with particle diameter, as measured (Tavman, 1996); particle diameter does not appear directly in the present theory, but the relative gap roughness does, and this decreases with particle diameter for constant surface condition. Similar agreement was found in the previous work (Lund, et al., 1997), but there deformation contact was required for that, more restrictive, correlation.

For magnesium oxide (MgO) particles in helium and air ($d_p = 0.2$ mm, $\varepsilon = 0.42$), Deissler and Boegli (1958) measured effective conductivities for various temperatures, as compared to the present theory in Figure 8; assuming a 0.25% gap between the 0.2 mm particles, there is excellent agreement with

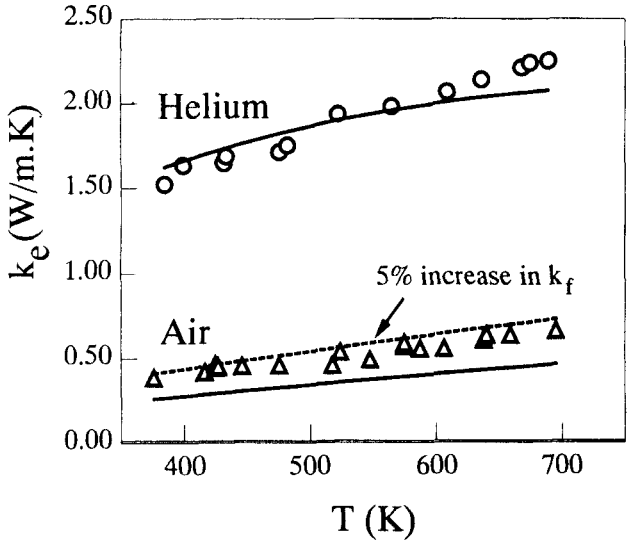

Figure 8 — Comparison with MgO data (δ_g = 0.25%).

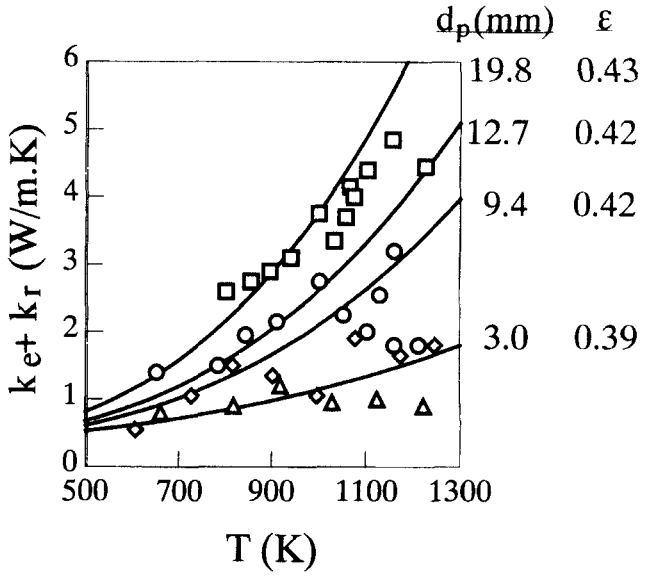

Figure 9 — Comparison with high-temperature data (δ_g = 0.1%).

the measurements for helium, but for air, the measurements exceed the calculations somewhat. Because of the small particle size, radiation is insignificant, even at 700 K. These experiments were conducted on the same particle-bed, but for different gases flushed through the bed; therefore, the same agreement for different gases (or lack of agreement) would be expected. However, if traces of residual helium remained in the bed, then the air conductivity could easily be higher than standard; this possible effect is modeled in Figure 8 by a 5% increase in the fluid conductivity, and shown as the dashed line. Or, if the void fraction changed from run to run, differences in k_e would result, as shown in Figure 7; experience shows that this fraction for the very same particles, gas and apparatus easily varies by ± 7% for different loadings. Similar results (i.e., close agreement with the helium data, and not-so-close with other gases) were obtained for the 446 stainless steel measurements (Deissler and Boegli, 1958).

High-temperature effective conductivities were determined by Huber and Jones (1988) for large, alumina spheres in air, as shown in Figure 9. At these high temperatures and large spheres, radiation is the dominant mode of heat transfer, which is modeled here by adding a radiation conductivity component: $k_e + k_r$. This component is adapted from the scattering theory of Kamiuto (1991), with γ as an effective scattering factor:

$$k_r = 4 d_p \gamma \sigma T^3;$$

$$\gamma = \frac{8/9}{(1+4\rho/9)(1-\varepsilon)[1+3(1-\varepsilon)-1.5(1-\varepsilon)^2]} \quad \cdots (5)$$

where ρ is the particle surface reflectivity.

In Figure 9 the solid lines represent computations from Equations (4) and (5), with a gap of δ_g = 0.1% and blackbody radiation, and with the void fractions and properties corresponding to the experimental data. Although the data in Figure 9 is quite scattered, there is quite good agreement between calculations and measurements. Indeed, Huber and Jones (1988) conclude that there is not quantitative agreement of their data with the model of Yagi and Kunii (1957), which considerably under-predicts the data; however, in terms of the present model, their measurements appear quite accurate (if not precise). Because of the high temperatures and the large particles, the total effective bed conductivity depends more on Equation (5) than on Equation (4); however, the comparison shows the validity of combining the radiative and conductive terms.

All of the above experiments have comparatively loose packings, and utilization of non-zero deformation contact, δ_c, was not required for agreement of the theory with experiment. However, in applications where the bed is either mechanically loaded or weighted by a tall column of particles, contact deformations will occur, with the attendant increase in the bed conductivity. This effect is included in the present correlation, and can be evaluated along with the Hertz deformation.

Conclusion

A detailed numerical conduction model was constructed to assess the effective bed conductivity. The finite element model of two particles in close proximity included an asperity interface gas gap of up to 0.5% of d_p, and deformation contact diameter ratio of up to 10%. The FE results clearly indicated that the majority of heat transfer takes place at or near the particle-particle contact point, whether there is actual contact at a particular instance or not. Calculations were performed for a wide range of conductivity ratios less than one, and a general correlation obtained for a wide range of fluid/solid conductivity ratios.

The numerical FE data were correlated in terms of a micro-asperity fluid gap, a deformation contact diameter, and solid and gas conductivities. By considering several packing arrangements, the effective conductivity was additionally determined as a function of void fraction, in general correspondence with published correlations. For typical fluid gaps between micro-rough particle surfaces there was excellent agreement with published measurements for both large and small particles in various gases over a wide temperature range.

Nomenclature

a-d = regression parameters
d_c = deformation contact diameter, (m)
d_p = particle diameter, (m)

F = nondimensional conductance, $K/d_p k_s$
g = *interface gap due to* asperities, (m)
K = calculated particle-particle conductance, (W/K)
k_e = effective bed conductivity, (W/m·K)
k_f = fluid conductivity, (W/m·K)
k_r = radiation conductivity, (W/m·K)
k_s = solid conductivity, (W/m·K)
m = packing parameter
Q = overall particle-particle heat flow, (W)
q'' = diametrical plane axial heat flux, (W/m^2)
R = calculated particle-particle resistance, $1/K$ (K/W)
T = temperature, (K)

Greek letters

δ_c = deformation contact diameter ratio, (d_c/d_p)
δ_g = asperity gap ratio, (g/d_p)
ε = void fraction
γ = effective radiative scattering constant
ρ = particle surface reflectivity
σ = Stefan-Boltzman constant

References

Balakrishnan, A. and D. C. T. Pei, "Heat Transfer in Gas–Solid Packed Bed Systems. 2. The Conduction Mode", Ind. Eng. Chem. PDD **18**, 1, 40–46 (1979).

Batchelor, G. K. and R. W. O'Brien, "Thermal or Electrical Conduction Through a Granular Material", Proc. R. Soc. A. (London) **355**, 313–333 (1977).

Baur, R. and E. U. Schluender, "Effective Radial Thermal Conductivity of Packings in gas flow. Part II. Thermal Conductivity of the Packing Fraction Without Gas Flow", Int. Chem. Eng. **18**, 2, 189–204 (1978).

Chan, C.K. and C. L. Tien, "Conductance of Packed Spheres in Vacuum", J. Heat Trans. **95**, 302–308 (1973).

COSMOS/M , Structural Research Analysis Corp., Los Angeles, CA.

Deissler, R. G. and J. S. Boegli, "An Investigation of Effective thermal Conductivities of Powders in Various Gases", Trans. ASME, 1417–1425(1958).

Dixon, A. G., "Thermal Resistance Models of Packed-Bed Effective Heat Transfer Parameters", AIChE J. **31**, 5, 826–834 (1985).

Fukai, Jun et al., "Simultaneous Measurement of Thermal Conductivity and Diffusivity by Periodic Heating of a Hot Wire", Heat Trans. Jap. Res. **19**, 4, 331–345 (1990).

Gorbis, Z.R. et al., "Analysis of Wall-Packed-Bed Thermal Interactions", Fusion Eng. Des. **27**, 216–225 (1995).

Hayashi, S. et al., "A Theoretical Model for the Estimation of the Effective Thermal Conductivity of a Packed Bed of Fine Particles", Chem. Eng. J. **35**, 51–60 (1987).

Huber, M. L. and M. C. Jones, "A frequency response study of packed bed heat transfer at elevated temperatures", Int. J. Heat Mass Trans. **31**, 4, 843–852 (1988).

Kamiuto, K., J., "Examination of Bruggeman's Theory for Effective Thermal Conductivities of Packed Beds", Nucl. Sci. Tech. **27**, 5, 473–476 (1990).

Kamiuto, K., J., "Analytical Expression for Total Effective Thermal Conductivities of Packed Beds", Nucl. Sci. Tech. **28**, 12, 1153–1156 (1991).

Kaviany, M., "Principles of Heat Transfer in Porous Media, 2nd Ed.", Springer Verlag, New York, NY (1995).

Krupiczka, R., "Analysis of Thermal Conductivity in Granular Materials", Int. Chem. Eng. **7**, 1, 122–144 (1967).

Kulkarni, B. D. and L. K. Doraiswamy, "Estimation of Effective Transport Properties in Packed Bed Reactors", Catal. Rev. Sci. Eng. **22**, 3, 431–483 (1980).

Lemcoff, N. O. et al., "Heat Transfer In Packed Beds," Rev. Chem. Eng. **6**, 4, 229–292 (1990).

Lund, K. O., Lord, S. M. and C. Thompson, "Microcontact Effects on Conduction in Packed Beds for Large Solid/Fluid Conductivity Ratios", Proc. AIChE Annual Meeting, Los Angeles, CA, Nov. 16–21, 103–107 (1997).

McPhedran, R. C. and D. R. McKenzie, "The Conductivity of Lattices of Spheres, I. The Simple Cubic Lattice", Proc. R. Soc. A. (London) **359**, 45–63 (1978).

Melanson, M. M. and A. G. Dixon, "Solid Conductivity in Low d_t/d_p Beds of Spheres, Pellets and Rings", Int. J. Heat Mass Trans., **28**, 2, 383–394 (1985).

Mingjie, Xu et al., "Thermal Conductivity of a Beryllium Gas Packed Bed", Fusion Eng. Des. **27**, 240–246 (1995).

Specchia, V. et al., "Heat Transfer in Packed Bed Reactors with One Phase Flow", Chem. Eng. Comm. **4**, 361–380 (1980).

Tavman, I. H., "Effective Thermal Conductivity of Granular Porous Materials", Int. Comm. Heat Mass Trans. **23**, 2, 169–176 (1996).

Wakao, N. and K. Kato, "Effective Thermal Conductivity of Packed Beds", J. Chem Eng. Japan **2**, 1, 24–33 (1969).

Yagi, S. and D. Kunii, "Studies on Effective Thermal Conductivities in Packed Beds", AIChE J. **3**, 373–381 (1957).

Yovanovich, M. M., "Thermal Contact Resistance Across Elastically Deformed Spheres", J. Spacecraft and Rockets **4**, 1, 119–122 (1967).

Manuscript received October 15, 1998; revised manuscript received March 23, 1999; accepted for publication April 21, 1999.